**Proceedings of the ASME 2020 International Design Engineering Technical Conferences & Computers and Information in Engineering Conference**
**IDETC/CIE 2020**
**August 16-19, 2020, St. Louis, USA**

**DETC2020-17855**

# DRAFT: GENERATIVE INFILLS FOR ADDITIVE MANUFACTURING USING SPACE-FILLING POLYGONAL TILES

**Matthew Ebert***
J. Mike Walker '66 Department of Mechanical Engineering
Texas A&M University
College Station, Texas 77843, USA

**Sai Ganesh Subramanian**†
J. Mike Walker '66 Department of Mechanical Engineering
Texas A&M University
College Station, Texas 77843, USA

**Ergun Akleman**‡
Department of Visualization
Texas A&M University
College Station, Texas 77843, USA

**Vinayak R. Krishnamurthy**
J. Mike Walker '66 Department of Mechanical Engineering
Texas A&M University
College Station, Texas 77843, USA

## ABSTRACT

*We study a new class of infill patterns, that we call wallpaper-infills for additive manufacturing based on space-filling shapes. To this end, we present a simple yet powerful geometric modeling framework that combines the idea of Voronoi decomposition space with wallpaper symmetries defined in 2-space. We first provide a geometric algorithm to generate wallpaper-infills and design four special cases based on selective spatial arrangement of seed points on the plane. Second, we provide a relationship between the infill percentage to the spatial resolution of the seed points for our cases thus allowing for a systematic way to generate infills at the desired volumetric infill percentages. Finally, we conduct a detailed experimental evaluation of the of these four cases to study their mechanical behavior under tensile loading.*

*Email: matt_ebert@tamu.edu
†Email: sai3097ganesh@tamu.edu
‡Email: ergun.akleman@tamu.edu
Email: vinayak@tamu.edu, Address all correspondence to this author.

## 1 Introduction

In this paper, we present a geometric modeling methodology for generating a new class of infills for additive manufacturing. Our methodology combines two fundamental ideas, namely, wallpaper symmetries in the plane and Voronoi decomposition to allow for enumerating material patterns that can be used as infills.

### 1.1 Motivation & Objectives

Generation of infills is an essential component in the additive manufacturing pipeline [1, 2] and significantly affects the cost, performance, and time to manufacture parts [3,4]. With increasing access to such extrusion based printers, the influence of infill patterns becomes more relevant. Studies also helps us optimize the print design based on production cost and time of 3D printed parts [5]. There are a only handful of infill patterns, such as hexagonal (honeycomb), quad-grid (square and diamond), and triangular, that are most commonly used in 3D printing. There are two challenges that motivate our work. First, while the known infill patterns have been extensively used, studied, and evaluated


Copyright © 2020 by ASME

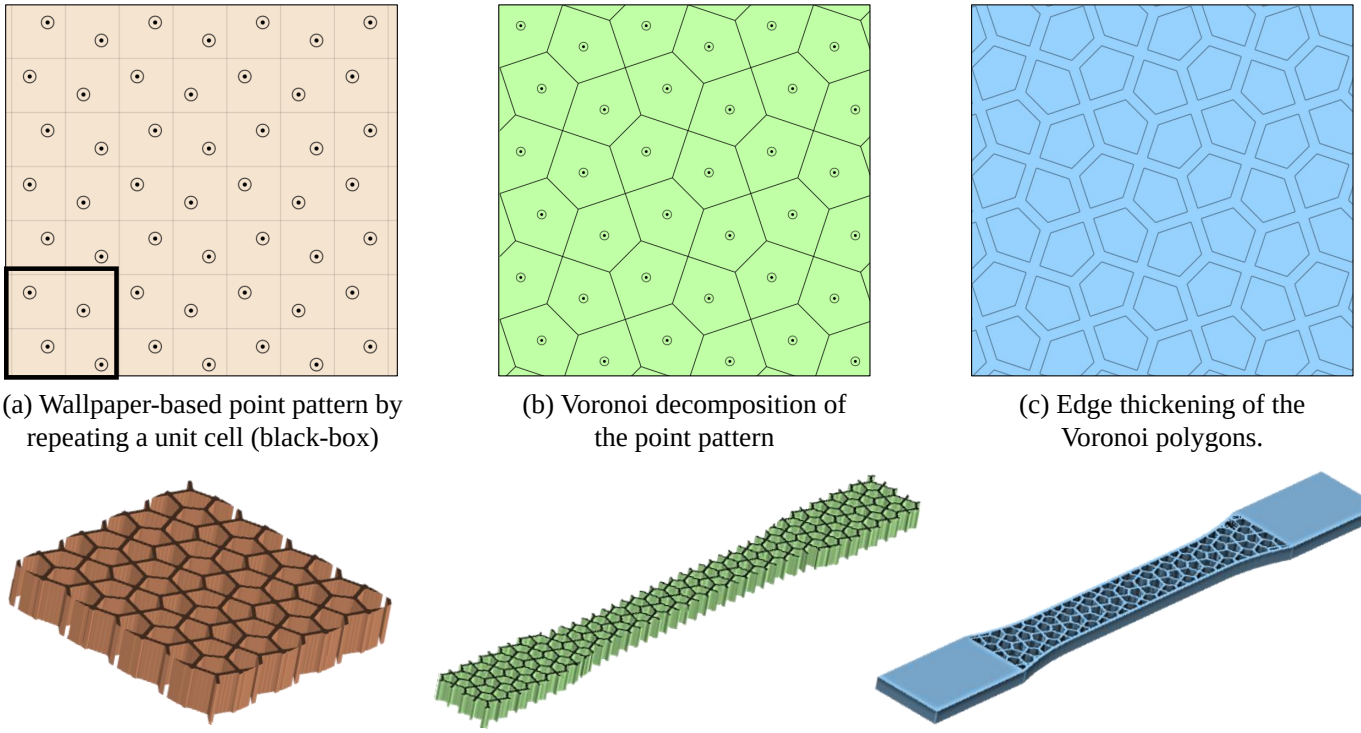

(a) Wallpaper-based point pattern by repeating a unit cell (black-box)

(b) Voronoi decomposition of the point pattern

(c) Edge thickening of the Voronoi polygons.

(d) Extrusion of the thickened boundary to obtain infill volume

(e) Infill volume trimming using the boundary a geometric model (dog-bone)

(f) Final geometry of dog bone. The top layer is removed to show the infill

**FIGURE 1**. The process of obtaining infill for a given input set of points and a wallpaper symmetry group. We demonstrate the process for regular Pentagonal tiling with p4g Wallpaper symmetry group

in literature [6, 7], there is currently no overarching methodology to design new infills. Second, even if such a methodology existed, the exploration of the geometric design space of infill patterns still needs to be tied to the physical characteristics that will result from those patterns.

Our objectives in this research are to (1) develop a generalized design methodology that allows one to search a vast space of geometric patterns for infill, (2) design a set of new infill pattern varieties to demonstrate the methodology in action, and (3) investigate the mechanical properties of these varieties to initiate future exploration of a more principled approach for predicting the geometry-mechanics relationship.

### 1.2 Rationale & Approach

Geometrically, the problem of designing infills is closely tied to the problem of finding regular shapes that could be used to fill 3D volumes. A space-filling polyhedron is a polyhedron that can be used to fill the entire 3-space by rigid body transformations, i.e. rotation, translation, and/or reflections [8]. This notion can be equivalently applied to any shape in general that can tessellate a given space simply through rigid transformation [9]. Therefore, a method to systematically generate polyhedra that are guaranteed to be space-filling would naturally allow for enumerating the design space of a wide variety of infill patterns. Our basic approach starts with the observation instead of enumerating space filling polyhedra through geometric heuristics, one may elegantly obtain such shapes simply by re-formulating the problem as a space-decomposition problem. Therefore, we propose the use of Voronoi decomposition as a central approach in our methodology. Earlier works have also used this idea for artistic explorations such as ornamental design [10], fractal patterns [11], and Escher designs [12]. Recently, Subramanian et al. [13] built upon Kaplan's approach by infusing wallpaper symmetries to generate a wide variety of 3D tilable shapes, known as Delaunay Lofts. Inspired by these works, We combine the idea of Voronoi decomposition (that guarantees space-filling shapes) along with wallpaper symmetries (that allows a systematic exploration of the pattern design space with simple input).

### 1.3 Contributions

We make the following contributions in this work:

1. We develop a geometric modeling approach for the design


Copyright © 2020 by ASME

of extruded infill patterns. For this, we combine the idea of wallpaper symmetries with Voronoi decomposition to generate space-filling shapes that tile 2-space [14]. We show a simple implementation of our approach using a well-known generative modeling tool. Unlike current approaches in Voronoi-based additive manufacturing algorithms, our unique combination offers a systematic approach to explore the design space of extruded infill patterns. Therefore, an infill pattern is simply instantiated using a 2D point distribution according to a chosen wallpaper symmetry. In fact, some of the common extruded infills (hexagonal, square, and diamond) are essentially special cases of wallpaper-infills generated by specific point arrangements in the plane.

2. Using our methodology, we demonstrate the design of four new infill patterns. We specifically showcase two well-known uniform patterns based on the Cairo pentagonal tiling of 2-space, a uniform quadrilateral pattern, and a non-uniform pattern that admits quadrilateral and pentagonal cells to fill 2-space. We investigate the geometric relationship between the infill percentage (which is an essential input parameter) to the geometric resolution (that is used in our algorithm to compute a pattern) and provide a numerical relationship between the two.
3. We conduct an in-depth experiment to characterize the structural properties of our four infill designs. Our experiments reveal some interesting insight into how the the shape of the unit cell in each pattern contributes to the trade-off between the ultimate tensile strength and plastic elongation. We show that our designed infills provide a wide range of elongation that depends on the degree-of-freedom associated with the space-filling polygon generated by a given wallpaper symmetry. Through the four cases, we demonstrate how the variation of the degrees-of-freedom within an infill pattern will ultimately vary the effective plastic deformation with the same amount of material consumption.

## 2 Related Works

Broadly speaking, the modeling, design, analysis, and manufacturing of patterned materials has been investigated in several different domains including design for additive manufacturing, computer graphics and geometric modeling, and mechanics. Here, we present a summary of selected works that broadly characterize the research in this area.

### 2.1 Voronoi Decomposition in Fabrication

Voronoi decomposition is a well-known and conceptually simple idea that can be used to generate a wide range of procedural patterns. This fact has been extensively used in several works for fabricating a wide variety of structures. A seminal example is the generation of procedural foams [15, 16]. Using Voronoi decomposition for creating 3D patterns have been expanded to 2.5D and 3D as well [13, 17]. For instance, Icking et al. [18] used 3D Voronoi diagrams based on polyhedral distances to develop structures for additive manufacturing with anisotropic behaviour. This work, however, is focused on generating infill patterns that allows material to withstand uneven and directional loads and offer more varied designs. There have been many attempts [19] after Icking et al. to explore more systematic applications of 3D Voronoi decomposition.

Voronoi decomposition gives us a planar straight line graph with a set of Voronoi vertices and connected by edges that are straight line segments. These edges make a planar rod network that has interesting mechanical characterisation. Recently, there has been interest in the mechanical characterization of a 3D printed 2D tiling in the context of "sheet materials" as well [20,21]. Schumacher et al [20] developed a numerical homogenization model to predict macroscopic deformation of structured sheet materials. Subsequently, it was extended to designing metamaterials (where the micro-structures are in a much smaller scale compared to the volume they fill) using star-shaped metric [21]. Finally, Voronoi diagrams offer different levels of flexibility to the design space. For example, in addition to Euclidean distance metric (or L2 norm) that is usually used, we can extend the design space by varying the distance metric [22] to $L_p$ norm, manhattan distance metric, weighted distance [23] and higher order Voronoi diagrams [24, 25].

### 2.2 Structure Modeling in Additive Manufacturing

The exploration of cellular, frame, and lattice structures has a rich history in additive manufacturing [26]. Early works on cellular structures have explored based on the process-structure-property-behavior model [27, 28]. One specific work worth noting is that by Rosen [29] that considers structural design for additive manufacturing from a broad methodological perspective. Similarly, several approaches for frame-like structures have been explored using conformal trusses [30] and skin-frame structures [31]. Finally, lattice based methods seek to provide geometric design approaches for procedural generation of structures for additive manufacturing processes [32]. Recent work by Zhang et al. demonstrates functionally graded lattice structures [33].

Prior works have also focused on generating generalized infill algorithms for inner support structure for 3D printing. Three-dimensional block partitioning based on an extension of 2D pattern method was studied [34] by dividing a given object using arbitrary planes to obtain blocks. Application-oriented optimizations are also developed for infill design. Recently, several in-fill patterns are developed using a bio-inspired approach [35]. For example, useful properties from porous structures can be lightweight as well as exhibiting strong mechanical properties which can be used to generate infills for additive manufacturing [36].


Copyright © 2020 by ASME

### 2.3 Physical Characterization of Infills

We can find several works in geometric design [37] and materials [38–40] that aim to study the mechanical (or in general physical) properties induced by the structure itself. However, in the context of infills, there are only a few selected works. For example, Fernandez et al. [41] and Dudescu and Racz [6] appear to be recent, yet initial works that systematically study the common infill patterns (triangular, rectilinear, full honeycomb, fast honeycomb, and wiggle grids) and infill parameters such as infill density. Our experimental methodology is based on this and other similar works [42] that have experimentally studied the mechanical response of 3D printed specimens.

### 2.4 Our Work

There are two main differences between our work and the current literature. First, our focus in this paper is to explore the space of infills extruded out of 2D space-filling tilings, as is common in current practice. The main reason is that 2D space-filling shapes have a more well-explored history in geometric analysis literature in comparison to 3D space-filling polyhedra. Furthermore, extruded infills are simple to construct as compared to the recently popular gyroid infills. Second, most of the previous works have used a stochastic algorithm to sample points locally and generate the Voronoi graph embedding in 2D or 3D [16,19]. In these works, Voronoi edges are further thickened to obtain the beam structure. Our goal, however, is to take a complementary approach provided by wallpaper symmetries that are more conceptually simple, offer intuitive exploration of the pattern space, and can be properly investigated from a mechanical standpoint. We believe this will help us better understand the mechanical behaviour of simple Voronoi patterns which may serve as the fundamental building blocks for developing complex micro-structures.

## 3 Theoretical Framework

### 3.1 Space-filling Polyhedra & Voronoi Decomposition

Space-filling polygons (2D) and polyhedra (3D) have been studied since the time of Plato with the aim of characterizing all possible shapes that could fill space (either 2D or 3D). To this effect, many works [43–47] attempted to determine if there were any Platonic solids other than cubes to fill-space as a uniform tiling. This, however, was shown to be impossible by Gardner [44]. Only eight convex polyhedra are known to be space-filling, of which only five have regular faces. These are the triangular prism, hexagonal prism, cube, truncated octahedron [48,49], and Johnson solid gyrobifastigium [50, 51].

Given the layered process of additive manufacturing, our focus in this paper is on prisms since these are extrusions of 2D tiles. In 2-space the only regular polygons that tile the space are equilateral triangle, a regular hexagon, and square. However, several other types of tilings have been enumerated in literature [52–55]. Two interesting cases of 2D tilings relevant to our approach are those presented by Kaplan [10] and Rao [56]. Kaplan demonstrated a simple yet powerful approach for creating a wide variety of artistic patterns. His main idea was to start with a set of points in the plane arranged in specific ways and then use these points as sites for Voronoi decomposition of the plane. Rao showed a systematic construction of 2D pentagonal tiling based on a similar approach.

In both these cases, the first critical observation is that if the Voronoi sites are arranged according to a certain symmetry, the resulting Voronoi decomposition provides an elegant method for partitioning space with at least semi-regular tiling. The second critical observation we make is that, this approach guarantees that the combination of unique Voronoi polygons resulting from the decomposition are space-filling. This is simply because of the fact that the Voronoi method, by definition, decomposes a whole space into parts that fit together. We leverage these two observations together to create a systematic methodology for enumerating different potential internal structures for additive manufacturing.

### 3.2 Wallpaper Symmetries

Wallpaper symmetries provide a mathematical categorization of all possible 2D repeating patterns by using simple operations like shifting, turning and flipping. The list of all symmetry groups identified are named as *p1, p2, p4, pm, pmm, p4m, p4m, cm, cmm, pg, pmg, pgg, p4g, p3, p6, p3m1, p31m* and *p6m* [57]. The first letter in the notation is either *'p'* or *'c'* signifying a primitive cell or face-centered cell. The successive number in the notation indicates number of folds of rotational symmetries applied. For example, in this work we have used *p4* symmetry, meaning the symmetric pattern is applied on a primitive with a 4-fold rotational symmetry. The next two symbols indicate other symmetry patterns that are incorporated.

Interestingly, irrespective of the type of symmetry we use a rectangular fundamental domain can be used to represent any symmetric pattern in 2D [58, 59]. Computer algorithms for Frieze groups (2D surface repeating in one direction) and Wallpaper patterns have been developed in Euclidian and affine spaces and even extended to describe patterns that are deformed under affine transformations [60]. This is the key observation that provides an intuitive method to generate all wallpaper symmetries simply by using affine transformations.

## 4 Methodology

The geometric design methodology for wall-paper-infills is based on three main steps: (1) create a 2D point-set configuration using wall-paper symmetries, (2) compute Voronoi decomposition using the point-set and then thicken the edges, and (3) extrude the resulting thick edges to construct our volume.


Copyright © 2020 by ASME

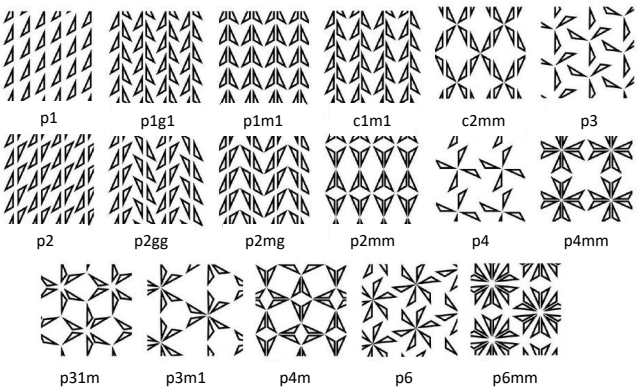


**FIGURE 2**. These are the 17 wallpaper symmetry groups that obtained for a triangular shape [61]

### 4.1 Computing Wallpaper Infills

**4.1.1 Generating Voronoi Sites** In order to make use of wallpaper symmetries, we begin with a rectangular decomposition of a rectangular region of 2-space which we call our *fundamental domain*. Subsequently, we select a neighborhood of cells in this decomposition (see the four neighboring cells in Figure 1(a)) and initialize points at the center of each of these cells. Then, we apply rigid transformations (rotation, translation, reflection) to the points in this neighborhood. These transformations are equivalent to instantiating a given wallpaper symmetry. Finally, we repeat this distribution throughout the remaining empty cells in the rectangular decomposition (Figure 1(a)).

**4.1.2 Voronoi Decomposition & Thickening** Given a 2D point pattern, we first compute the Voronoi decomposition of this pattern (Figure 1(b)). This gives us a set of space-filling polygons corresponding to each point in the set. Finally we thicken the Voronoi edges by using the level-sets of the implicit distance function with the Voronoi edges as the control geometry. For this, we build an implicit function in our fundamental domain that is given by the distance of a point in the domain to the closest Voronoi edge.

In principle, once the 2D regions are computed, it is simple to extrude the region using any known geometric modeling method such as a mesh-based or a volumetric approach.

### 4.2 Infill Design

**4.2.1 Pattern selection** Using Wallpaper symmetry as a tool we can generate a number of patterns. We specifically make use of p4g and p4 symmetry groups for the patterns. Based on our exploration we zeroed down upon 4 patterns to explore.

The first pattern we explored is a pentagonal voronoi tessellation. There are fifteen different types of convex pentagons currently identified to tile a plane including a recent discovery in

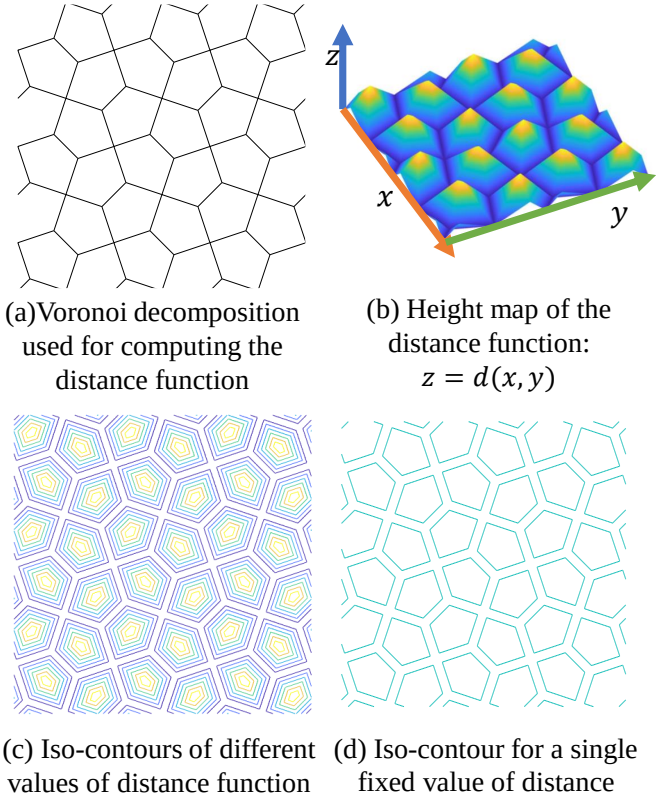


(a)Voronoi decomposition used for computing the distance function

(b) Height map of the distance function: $z = d(x, y)$

(c) Iso-contours of different values of distance function

(d) Iso-contour for a single fixed value of distance

**FIGURE 3**. The iso-offset surface and contour plots generated from the Voronoi decomposition. Varying the distance $z$ would give us the edge loops for various infill densities

2015 [56]. Of these the isoperimetric pentagonal tiling [62] has a special relationship with the hexagonal pattern as it can be seen as a union of two hexagonal tilings as well. The dual of this tiling is a snub square consisting of squares and triangles [63]. Thus, we observe that these tilings can indeed be constructed using a 2D Voronoi tessellation with some sort of patterns.

First two shapes that we consider are made from p4g group of Wallpaper symmetry. Assume a square tile with 4-fold rotational symmetry and its mirror image. This symmetry group can be understood as a grid of this square tile with appropriate spacing. The first two shapes are two instances of the same type of symmetry group with a different orientation.

The other two shapes are made from p4 Wallpaper symmetry group. This can simply be understood as grid patterns of squares with 4-fold symmetry. We chose two points in a particular orientation and then apply the p4 transformation to get the tiling. The third shape is a semi-regular tiling that consists of two different shape that together tile the 2D Space. The other shape is a similar equivalent of Cairo tiling, in the sense that this tiling can be seen as a union of hexagonal tilings as well. However, the fundamental repeating shape is a special type of cyclic quadrilateral. Please


Copyright © 2020 by ASME

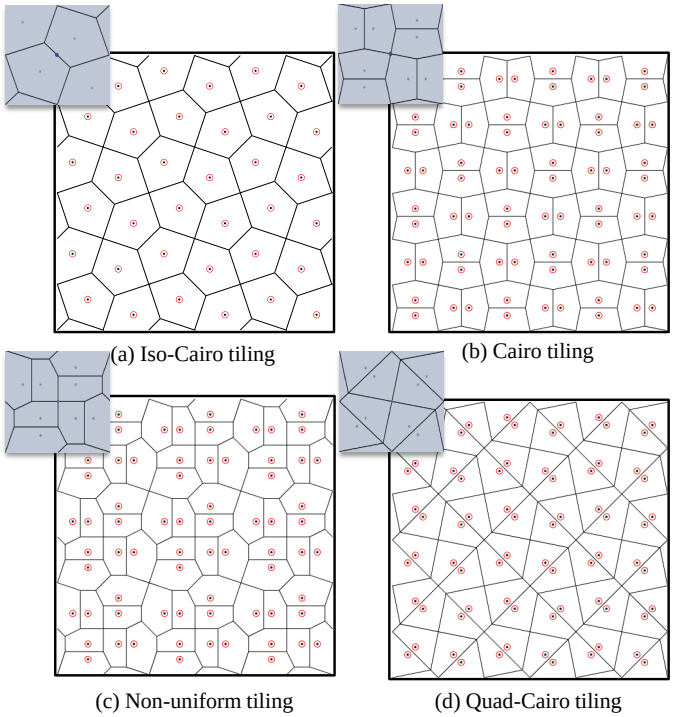


**FIGURE 4**. These are the four Voronoi patterns that we consider in this paper to base our infill pattern design. The blue dot in the center is the point about which the 4-fold rotations are applied to the shapes.

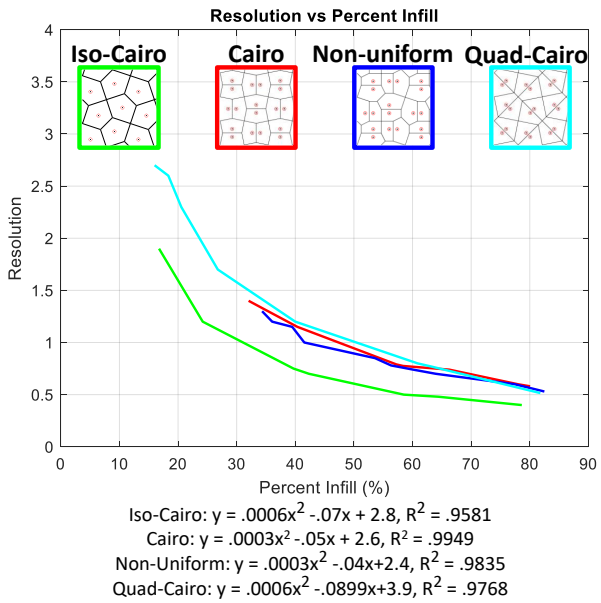


**FIGURE 5**. The plot shows the resolution as a function of infill percentage. Here resolution is the size of one repeating unit tile. As infill increases the size of one repeating unit block must become smaller.

refer to figure 4 for the representation of the repeating square for the 4 cases we consider.

Although we use a specific symmetric pattern to generate the required tilings, there can be more than one way to obtain a same set of point groups using different wallpaper groups. In fact, these symmetry groups are classified based on simple Euclidean plane transformation consisting of translation, rotation and flip operations. The user can simply assume any random set of input points, apply the transformation in a particular order and generate a variety of symmetric patterns.

**4.2.2 Infill density control** Another important design parameter specific to 3D printing is infill density. Simply put, it is the ratio of volume of solid material to the volume of the object. While a very high infill density may suppress the characteristics of the infill pattern, an optimal infill density would help us to have a trade-off between plastic elongation and ultimate tensile strength. Thus it is important to be able to actively control the infill density of the 3D prints.

There are two ways in which we can control the infill density. We can either choose to increase/decrease the thickness of the iso-offsets or vary the resolution of the input points. The latter basically amounts to decreasing the lengths of the unit square we sample while maintaining a constant value of the offset distance. We choose this approach as it is more widely used in 3D Printing. However, the variation of in-fill density with respect to the resolution of the pattern is not a simple pattern and it varies with respect to the pattern in consideration.

It is important to note that shrinking the size of the unit tile does have effects on the internal structure. Since the iso-offset is kept as a fixed distance this creates problems when shrinking to very small unit tile sizes needed for 80% infills. Doing this does also create problems with non-identical tiles. For example the Non-Uniform structure contains two different types of shapes, while they are both pentagons the area contained within the two different shapes is not the same. This means that by shrinking the shape down to smaller sizes the area decreases the same amount in each shape but not proportionally. For example the larger shape could have a 50% reduction in area which when subtracting the same amount of area from the smaller shape results in 75% reduction in area.

## 4.3 Implementation

We used Houdini, a generative modeling software to create our infills. Our main objective was to generate these infills within a standard dog-bone specimen geometry. For that, we first generated a 3D infill pattern within a rectangular fundamental domain (Figure 1(d)) following which we compute an intersection between the infill and the pre-modeled dog-bone geometry to


Copyright © 2020 by ASME

obtain a trimmed internal infill structure (Figure 1(e)). Finally, we created our specimen by taking a union of a shelled version of the dog-bone model and the trimmed infill structure (Figure 1(f)). However, we maintained solid geometry of the dog-bone at the ends for ensuring structural integrity under clamping pressure from a universal testing machine.

To calculate the infill percentage of the structure we can determine the volume of a solid Dog-bone as well as the shelled volume. These two can be used as the maximum and minimum volumes which are linearly correlated with infill percentage. A final volume of the combined dog-bone is measured and an infill can be calculated based on a shelled dog-bone having 0% infill and a solid dog-bone having 100% infill.

## 5 Experimental Procedure

The goal of our experiment was to characterize the mechanical behavior of the four infill patterns under tensile loading. Specifically, we wanted to (a) determine the ultimate tensile stress, (b) study the stress-strain relationship under tensile loading, and (c) characterize how their mechanical behavior changes with respect to infill density. We also wanted to compare these patterns with each other in terms of their mechanical behavior.

### 5.1 Test Specimen Fabrication

In our experiments, we used the ASTM D638 Type 1 sample as the testing (dog-bone) specimen. All our test specimens were printed using the Monoprice Maker Select V2. We used a layer thickness of 0.2mm during the slicing of our 3D models of the test specimens. Another key factor that we considered was the amount of perimeter layers to create. Since the perimeter lines of material run parallel to the direction of the tensile loading in the structure, the amount of perimeter layers will have large effects on the Ultimate Tensile Stress [41]. To a similar degree the first few layers (top) and the last few layers (bottom) of a print are not usually characterized by their different infill patterns instead by a solid layer. For our testing and generation purposes all infill perimeters were fixed at two layers and there were four top and bottom layers. All slicing done for this paper is done using Ultimaker CURA.

For each of the four different types of dog-bone infill structures three total samples were tested. This ensures that a single sample was not an anomaly. We further ensured that all samples at the same infill were printed using the same roll of filament which eliminates the variable of two different spools, even from the same manufacturer having different properties. In doing so all samples at the same infill can be compared with one another.

### 5.2 Apparatus

For this, we conducted a sequence of tensile tests for each pattern with 20%, 40%, 60%, and 80 % infill density. All tests

g.

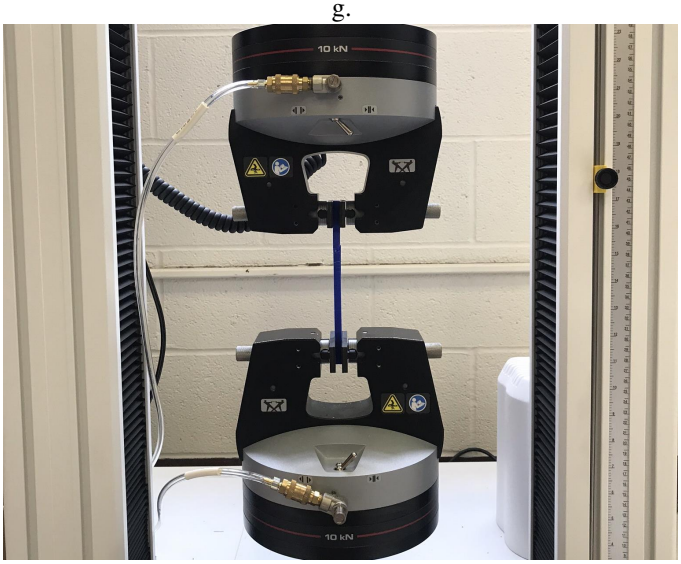


**FIGURE 6**. This shows the experimental setup for the testing apparatus. The sample in the testing apparatus was printed in blue and is currently being viewed from the side. There are pneumatic grips holding the sample in place.

were run on an Instron tensile tensile testing machine with a 10kN load cell (Figure 6). The machine grips the sample with pneumatic grips which apply an even 30PSI compressing force on the sample to hold it in place. The choice of grip load was based on maintaining the structural integrity of the sample while ensuring proper gripping. Each sample was tested at a pulling rate of 6mm/min. For each specimen, we collected force, displacement, stress, and percent elongation with given values of length and cross sectional area.

## 6 Results

### 6.1 Preliminary Tests with Honeycomb & Grid

In order to qualitatively compare our infills with commonly known patterns in practise, we conducted pilot tests to determine the ultimate tensile stress (UTS) and capture the stress-elongation relationship for the square grid and hexagonal (honeycomb) patterns. The ultimate tensile stress for grid pattern was near 15MPa and occurred at 2.1% elongation which is where it broke as well. The hexagonal pattern reached UTS at 2.1% elongation with a stress of 12.5 MPa and broke at 2.3% elongation and 11 MPa.

### 6.2 20% Infill Density

In the case of our own generated shapes we show that there exits several shapes that can have more plastic elongation than normal dog-bone structures with standard infill. This can be seen most notably in the percent elongation at break where the Iso-


Copyright © 2020 by ASME

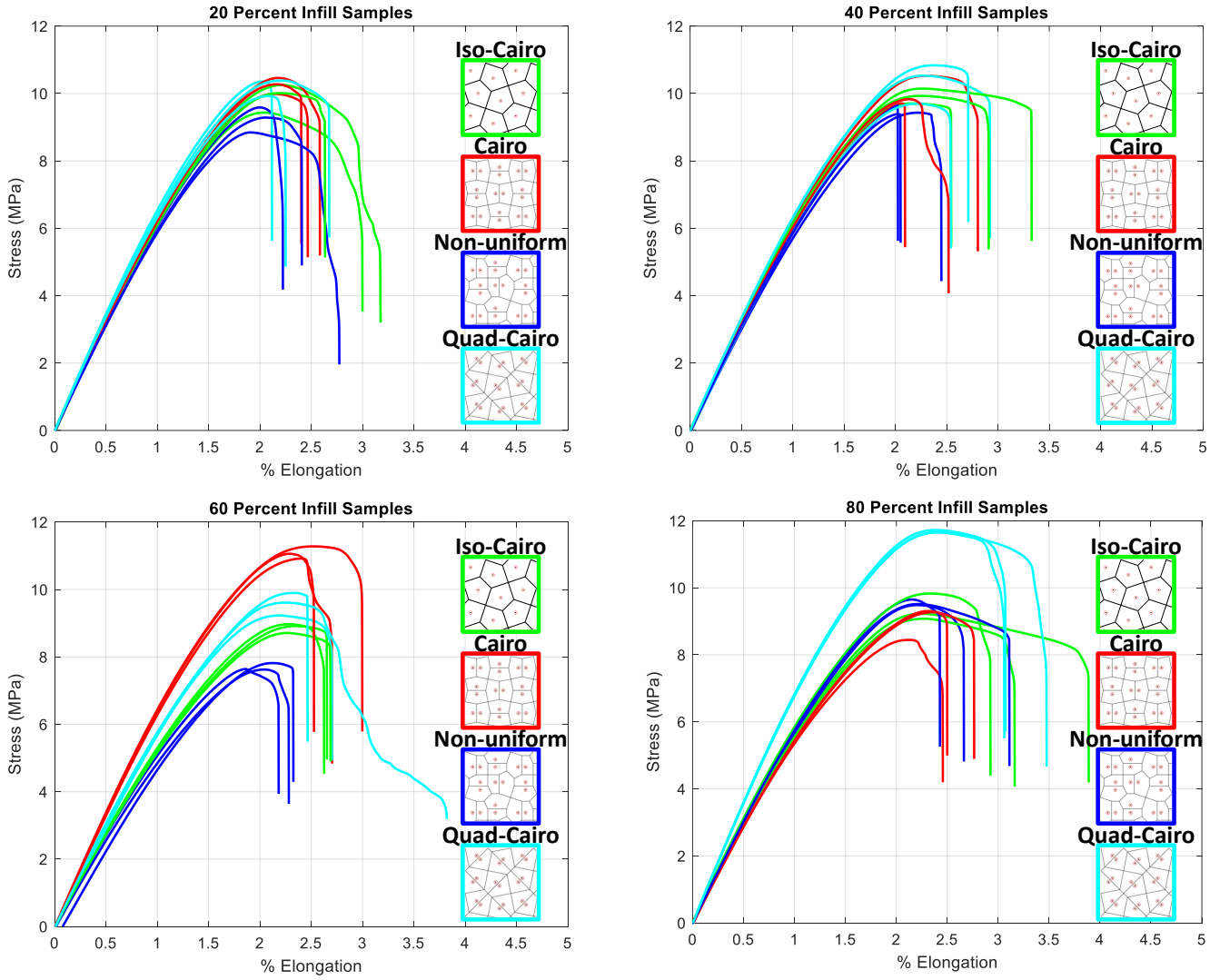


**FIGURE 7**. The stress-elongation plots for four different infill percentages with four different internal geometries at each infill. For each structure at each infill three samples were tested and the results of all of them are shown. Each plot is shown with the corresponding structure represented using the initial wallpaper shapes.

Cairo structure shows higher elongation than the next highest structure by a magnitude of 0.5% elongation(Table 1). As previously stated the elongation at the ultimate tensile stress (UTS) was all nearly equivalent at 2.1% elongation. When compared to the grid infill from our preliminary tests, the elongation change from UTS to the breaking point we observed that all our patterns generally admit a higher plastic elongation. However, this increase in plastic behavior does have a negative effect on the tensile strength of the material. In the case of Iso-Cairo there is a near 50% reduction in strength when compared with grid (UTS ˜15MPa). However there is also a 50% increase in the elongation of the material when comparing the breaking elongation where grid broke at around 2% elongation. We can also see that at this infill percentage of our tested structures, excluding Iso-Cairo, all exhibit similar elongation at break to the hexagonal structure that was tested in the preliminary testing phase. This leads to the conclusion that at 20% infill the Iso-Cairo shape exhibits more plastic deformation ability than both hexagonal infill as well as grid. Also note that all patterns behave similarly up until 1.5% elongation which indicates that at lower infill percentages the outside layers dominate stress behavior up until ultimate tensile strength.


Copyright © 2020 by ASME

### 6.3 40% Infill Structures

In the case of 40% infill we observed a greater disparity between elongation at UTS and breaking. This is most notably seen again in Iso-Cairo where there is a 1% elongation between when the material reaches the UTS and when it breaks (Table 1). With this information we can conclude that at 40% infill the best structure to use for the greatest plastic deformation is Iso-Cairo.

Similar to 20% infill up until around 1.5% elongation there is little difference between all of the structures stress. However after the sample reaches UTS there is a larger difference between the samples suggesting that at this infill percentage structures start to influence the stress behavior.

### 6.4 60% Infill Structures

At 60% infill the curve of each structure can be more easily generalized since they are very similar to each other, more so than the lower infill densities. This suggests that at 60% infill there exists a much stronger relationship between stress and the internal geometry. This shows that at 60% infill the geometry dominates the stress-elongation values and not the external structure.

It is important to note that while Iso-Cairo had the highest elongation at break at the smaller infills that is no longer the case. Instead Cairo and Quad-Cairo both have larger elongation at break than Iso-Cairo. This means that at each infill percentage a different pattern may be ideal for creating a material with high plastic deformation.

The most important observation we make is that at 60% infill, the UTS reduced for Iso-Cairo and Non-uniform patterns. This is counter-intuitive since an increase in material volume should typically lead to higher strength. However, our results show that this is not the case. In the Non-Uniform Structure the UTS went down from 9.48 MPa at 40% infill to 7.96 MPa at 60% infill. This is not a statistical anomaly since none of the Non-Uniform samples reached greater than 8 MPa ultimate tensile stress. This idea that UTS will go down with an increase in material is further confirmed at higher infill rates for Cairo shaped infills.

### 6.5 80% infill Structures

At 80% infill there is no longer four separate curves representing each structure. In fact the stress vs elongation lines are similar to that of 40% infill except in the case of Quad-Cairo. In the case of Quad-Cairo there is a clear difference from all other smaller infill densities where Quad-Cairo reaches much higher UTS and a higher percent elongation than other structures. Going from 60% infill to 80% in the Cairo shape shows a decrease of 2 MPa. This is more evidence that shows that ultimate tensile stresses do not always increases with an increase in material consumption.

| Pattern | UTS | Elongation at UTS | Stress at Break | Elongation at Break |
|---|---|---|---|---|
| **20% Infill Density** | | | | |
| Iso-Cairo | 9.8970 | 2.1522 | 6.5203 | 2.9305 |
| Cairo | 10.2379 | 2.1578 | 9.2698 | 2.4816 |
| Non-Uniform | 9.2370 | 1.9862 | 6.0352 | 2.4662 |
| Quad-Cairo | 10.2287 | 2.0972 | 9.2767 | 2.3979 |
| **40% Infill Density** | | | | |
| Iso-Cairo | 9.9277 | 1.9010 | 9.2191 | 2.9254 |
| Cairo | 10.0208 | 2.1671 | 8.5647 | 2.4703 |
| Non-Uniform | 9.4873 | 2.0929 | 8.8756 | 2.1729 |
| Quad-Cairo | 10.3544 | 2.2918 | 9.6212 | 2.7225 |
| **60% Infill Density** | | | | |
| Iso-Cairo | 8.8667 | 2.2993 | 8.0190 | 2.6530 |
| Cairo | 11.0862 | 2.3990 | 9.0482 | 2.7405 |
| Non-Uniform | 7.6942 | 2.0112 | 6.7489 | 2.2616 |
| Quad-Cairo | 9.5794 | 2.2570 | 7.0847 | 2.9933 |
| **80% Infill Density** | | | | |
| Iso-Cairo | 9.3771 | 2.2831 | 7.3295 | 3.3230 |
| Cairo | 9.0066 | 2.2657 | 7.9570 | 2.5712 |
| Non-Uniform | 9.5500 | 2.1875 | 8.5699 | 2.7312 |
| Quad-Cairo | 11.6804 | 2.3939 | 8.6175 | 3.1994 |

**TABLE 1**. The stress and elongation at ultimate tensile strength and at breaking point. All stresses are represented in MPa and all elongations shown are in %. These have been simplified into 20%, 40%, 60%, and 80% infill densities. The shown values are the averages of 3 samples at each infill and type.

## 7 Discussion

### 7.1 Degrees of Freedom

The results show that near the UTS there is very similar behavior regardless of the internal infill structure at 20% infill. Since the only constant thing between all four structures is their outside shell we can theorize that this outside shell dominates stress transfer and distribution. This is because up until the UTS point there is no infill structure that goes directly in the direction of the tension of the specimen. This is when the specimen is elastically deforming and the interior structures are deforming to align themselves with the direction of tension. This notion can be


Copyright © 2020 by ASME

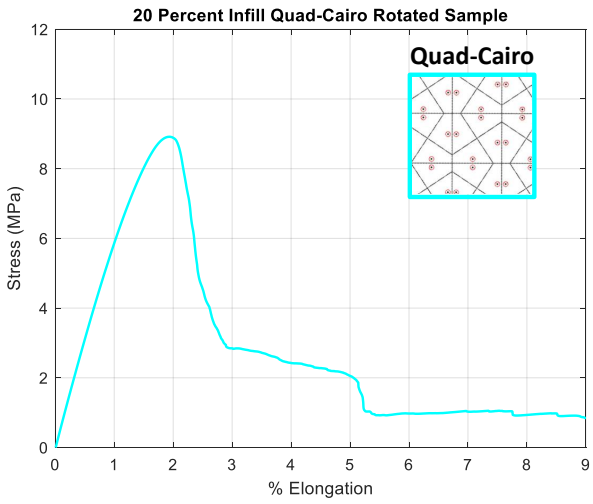


**FIGURE 8**. The stress-strain curve of the Caro-Quad pattern rotated by $45^o$ shows unusual behavior beyond the breaking point. Observe that the plastic strain extends significantly beyond the ultimate tensile strength from 2% elongation to 9%. We observed specific cells in the pattern that maintained the structural integrity even after breakage of the internal structure by-and-large,

associated with the idea of kinematic degrees-of-freedom wherein the shape of the space-filling polygon is related to the geometry of deformation of the structures.

This can also be seen in several of the preliminary results made where one sample at 20% infill was tested using grid and hexagon. In the case of grid the vertical lines are in the direct orientation of the tension. This gives it no degrees of freedom since there is no ability of the structure to deform and align itself more with the direction of tension. Therefore in this example the sample broke as it reached the UTS. In the case of hexagon there were several degrees of freedom within the structure which allows it to stretch, moving to 2.3% elongation before breaking, even after reaching UTS.

This particular aspect is an important direction of further study, particularly from the perspective of directional anisotropy. For example, we conducted a simple experiment wherein we subjected the Quad-Cairo pattern to tensile loading after a 45° rotation. We observed a significantly different behavior after UTS, (Figure 8). While the effect of infill orientation has been studied in the past, our methodology opens up a larger space of patterns that requires further studies.

### 7.2 Amount of Material Link to UTS

As shown in the Results an increase in material does not necessarily increase the UTS as seen in Non-Uniform structure when increasing from 40% to 60%. This is counter intuitive and is an idea that has not yet been shown in other material structures. In particular cases infill structures can increase in ultimate tensile stress, then at higher infill percentages can decrease again. This means that the mechanical behavior at these infill percentages are highly dependent on the geometry of the parts suggesting a deep relationship between these two characteristics. The reason why this occurs is unknown but needs more exploration on the topic.

### 7.3 Effective Plastic Behavior

It is known that highly plastic materials are desired while keeping a high UTS within a material [64]. We have shown that for some structures we are able to increase the percent elongation at breaking. Particularly there is a change in elongation at certain structures at specific infill densities. When compared with the elongation of normal infill structures our structures have shown great improvements on the elongation before breaking. Some wallpaper symmetry structures also only show highly plastic abilities at certain infill percentages suggesting that there is a great role in the geometry of the infill.

## 8 Conclusion

Our goal in this paper was to develop and investigate a geometric modeling methodology for generating infill patterns for additive manufacturing. To this end, we demonstrated an approach that combined wallpaper symmetries in conjunction with Voronoi decomposition to generate such infills. We further investigated four specific types of infill patterns using our methodology. Our experimental investigation reveals several key insights regarding how the geometry of the polygonal unit cells (degree of freedom of the polygon) affects the physical behavior. To that effect, we also demonstrated patterns that exhibit high elongation rates after the maximal stress has been reached. This can be particularly useful for applications that require more compliant behavior from printed parts.

There are several key questions that need further exploration. For instance, the patterns generated using our approach exhibit anisotropic behavior that should be geometrically characterized. One of our immediate future goals is to conduct a comparative analysis of our four cases with the currently known infill patterns. Secondly, the effect of an infill is also likely to change based on the bounding geometry of a part. This aspect needs to be further studied. Using our method, several studies are possible in the future to explore the intersection of infill pattern space and constitutive material properties, especially for flexible materials. We believe that this work could complement several seminal approaches that are currently exploring metamaterials [65] with properties such as negative stiffness [66, 67]. In conclusion, we believe that our methodology opens up new design space for infills and additive manufactured structured materials in general.


Copyright © 2020 by ASME

## ACKNOWLEDGMENT

This work was partially supported by the Texas A&M University start-up fund and the J. Mike Walker '66 Department of Mechanical Engineering at Texas A&M University, College Station. The authors also wish to thank Dr. Matt Pharr for providing access to the tensile testing equipment for this research.

## REFERENCES

[1] Livesu, M., Ellero, S., Martínez, J., Lefebvre, S., and Attene, M., 2017. "From 3d models to 3d prints: an overview of the processing pipeline". In Computer Graphics Forum, Vol. 36, Wiley Online Library, pp. 537–564.

[2] Seepersad, C. C., 2014. "Challenges and opportunities in design for additive manufacturing". *3D printing and Additive Manufacturing,* ***1***(1), pp. 10–13.

[3] Boyer, J., Seepersad, C., Simpson, T. W., Williams, C. B., and Witherell, P., 2017. "Designing for additive manufacturing recent advances in design for additive manufacturing". *Journal of Mechanical Design, Transactions of the ASME,* ***139***(10), p. 100901.

[4] Maconachie, T., Leary, M., Lozanovski, B., Zhang, X., Qian, M., Faruque, O., and Brandt, M., 2019. "Slm lattice structures: Properties, performance, applications and challenges". *Materials & Design*, p. 108137.

[5] Baich, L., Manogharan, G., and Marie, H., 2015. "Study of infill print design on production cost-time of 3d printed abs parts". *International Journal of Rapid Manufacturing,* ***5***(3-4), pp. 308–319.

[6] Dudescu, C., and Racz, L., 2017. "Effects of raster orientation, infill rate and infill pattern on the mechanical properties of 3d printed materials". *ACTA Universitatis Cibiniensis,* ***69***(1), pp. 23–30.

[7] Popescu, D., Zapciu, A., Amza, C., Baciu, F., and Marinescu, R., 2018. "Fdm process parameters influence over the mechanical properties of polymer specimens: A review". *Polymer Testing,* ***69***, pp. 157–166.

[8] Loeb, A. L., 1991. "Space-filling polyhedra". In *Space Structures*. Springer, pp. 127–132.

[9] Grünbaum, B., and Shephard, G. C., 1980. "Tilings with congruent tiles". *Bulletin of the American Mathematical Society,* ***3***(3), pp. 951–973.

[10] Kaplan, C. S., 2000. "Voronoi diagrams and ornamental design".

[11] Shirriff, K., 1993. "Generating fractals from voronoi diagrams". *Computers & graphics,* ***17***(2), pp. 165–167.

[12] Bachmeier, E. E., 2016. "Tessellations: an artistic and mathematical look at the work of maurits cornelis escher".

[13] Subramanian, S. G., Eng, M., Krishnamurthy, V. R., and Akleman, E., 2019. "Delaunay lofts: A biologically inspired approach for modeling space filling modular structures". *Computers & Graphics,* ***82***, pp. 73–83.

[14] Subramanian, S. G., Eng, M., Krishnamurthy, V. R., and Akleman, E., 2019. "Delaunay lofts: A biologically inspired approach for modeling space filling modular structures". *Computers & Graphics,* ***82***, pp. 73–83.

[15] Martínez, J., Dumas, J., and Lefebvre, S., 2016. "Procedural voronoi foams for additive manufacturing". *ACM Transactions on Graphics (TOG),* ***35***(4), pp. 1–12.

[16] Martínez, J., Song, H., Dumas, J., and Lefebvre, S., 2017. "Orthotropic k-nearest foams for additive manufacturing". *ACM Transactions on Graphics (TOG),* ***36***(4), pp. 1–12.

[17] Howison, M., and Séquin, C. H., 2009. "Cad tools for creating space-filing 3d escher tiles". *Computer-Aided Design and Applications,* ***6***(6), pp. 737–748.

[18] Icking, C., Klein, R., Ma, L., Nickel, S., and Weißler, A., 2001. "On bisectors for different distance functions". *Discrete applied mathematics,* ***109***(1-2), pp. 139–161.

[19] Martínez, J., Hornus, S., Song, H., and Lefebvre, S., 2018. "Polyhedral voronoi diagrams for additive manufacturing". *ACM Transactions on Graphics (TOG),* ***37***(4), pp. 1–15.

[20] Schumacher, C., Marschner, S., Gross, M., and Thomaszewski, B., 2018. "Mechanical characterization of structured sheet materials". *ACM Transactions on Graphics (TOG),* ***37***(4), pp. 1–15.

[21] Martínez, J., Skouras, M., Schumacher, C., Hornus, S., Lefebvre, S., and Thomaszewski, B., 2019. "Star-shaped metrics for mechanical metamaterial design". *ACM Transactions on Graphics (TOG),* ***38***(4), pp. 1–13.

[22] Aichholzer, O., Chen, D. Z., Lee, D., Mukhopadhyay, A., Papadopoulou, E., and Aurenhammer, F., 1997. "Voronoi diagrams for direction-sensitive distances". In Proceedings of the thirteenth annual symposium on Computational geometry, pp. 418–420.

[23] Balcázar, J. L., Díaz, J., and Gabarró, J., 2012. *Structural complexity II*, Vol. 22. Springer Science & Business Media.

[24] Cheong, O., Everett, H., Glisse, M., Gudmundsson, J., Hornus, S., Lazard, S., Lee, M., and Na, H.-S., 2007. "Farthest-polygon voronoi diagrams". In European Symposium on Algorithms, Springer, pp. 407–418.

[25] Reem, D., 2011. "The geometric stability of voronoi diagrams with respect to small changes of the sites". In Proceedings of the twenty-seventh annual symposium on Computational geometry, pp. 254–263.

[26] Helou, M., and Kara, S., 2018. "Design, analysis and manufacturing of lattice structures: an overview". *International Journal of Computer Integrated Manufacturing,* ***31***(3), pp. 243–261.

[27] Rosen, D. W., 2007. "Computer-aided design for additive manufacturing of cellular structures". *Computer-Aided Design and Applications,* ***4***(5), pp. 585–594.

[28] Chu, C., Graf, G., and Rosen, D. W., 2008. "Design for additive manufacturing of cellular structures". *Computer-Aided Design and Applications,* ***5***(5), pp. 686–696.


Copyright © 2020 by ASME

[29] Rosen, D. W., 2007. "Design for additive manufacturing: a method to explore unexplored regions of the design space". In Eighteenth Annual Solid Freeform Fabrication Symposium, University of Texas at Austin (freeform) Austin, TX, pp. 402–415.

[30] Wang, H., Chen, Y., and Rosen, D. W., 2005. "A hybrid geometric modeling method for large scale conformal cellular structures". In ASME 2005 International Design Engineering Technical Conferences and Computers and Information in Engineering Conference, American Society of Mechanical Engineers Digital Collection, pp. 421–427.

[31] Wang, W., Wang, T. Y., Yang, Z., Liu, L., Tong, X., Tong, W., Deng, J., Chen, F., and Liu, X., 2013. "Cost-effective printing of 3d objects with skin-frame structures". *ACM Trans. Graph.,* ***32***(6), Nov.

[32] Pasko, A., Fryazinov, O., Vilbrandt, T., Fayolle, P.-A., and Adzhiev, V., 2011. "Procedural function-based modelling of volumetric microstructures". *Graphical Models,* ***73***(5), pp. 165–181.

[33] Zhang, J. Z., Sharpe, C., and Seepersad, C. C., 2019. "Stress-constrained design of functionally graded lattice structures with spline-based dimensionality reduction". In International Design Engineering Technical Conferences and Computers and Information in Engineering Conference 59186, Vol. 59186, American Society of Mechanical Engineers, p. V02AT03A063.

[34] Lee, J., and Lee, K., 2017. "Block-based inner support structure generation algorithm for 3d printing using fused deposition modeling". *The International Journal of Advanced Manufacturing Technology,* ***89***(5-8), pp. 2151–2163.

[35] Podroužek, J., Marcon, M., Ninčević, K., and Wan-Wendner, R., 2019. "Bio-inspired 3d infill patterns for additive manufacturing and structural applications". *Materials,* ***12***(3), p. 499.

[36] Wu, J., Aage, N., Westermann, R., and Sigmund, O., 2017. "Infill optimization for additive manufacturing—approaching bone-like porous structures". *IEEE transactions on visualization and computer graphics,* ***24***(2), pp. 1127–1140.

[37] Zhao, H., Gu, F., Huang, Q.-X., Garcia, J., Chen, Y., Tu, C., Benes, B., Zhang, H., Cohen-Or, D., and Chen, B., 2016. "Connected fermat spirals for layered fabrication". *ACM Trans. Graph.,* ***35***(4), July.

[38] Decuir, F., Phelan, K., and Hollins, B. C., 2016. "Mechanical strength of 3-d printed filaments". In 2016 32nd Southern Biomedical Engineering Conference (SBEC), IEEE, pp. 47–48.

[39] Yarwindran, M., Sa'aban, N. A., Ibrahim, M., and Periyasamy, R., 2016. "Thermoplastic elastomer infill pattern impact on mechanical properties 3d printed customized orthotic insole". *ARPN Journal of Engineering and Applied Sciences,* ***11***(10), pp. 6519–6524.

[40] Moscato, S., Bahr, R., Le, T., Pasian, M., Bozzi, M., Perregrini, L., and Tentzeris, M. M., 2016. "Infill-dependent 3-d-printed material based on ninjaflex filament for antenna applications". *IEEE Antennas and Wireless Propagation Letters,* ***15***, pp. 1506–1509.

[41] Fernandez-Vicente, M., Calle, W., Ferrandiz, S., and Conejero, A., 2016. "Effect of infill parameters on tensile mechanical behavior in desktop 3d printing". *3D printing and additive manufacturing,* ***3***(3), pp. 183–192.

[42] Poudel, L., Sha, Z., and Zhou, W., 2018. "Mechanical strength of chunk-based printed parts for cooperative 3d printing". *SME North American Manufacturing Research Conference,* ***49***, pp. 962–972.

[43] Senechal, M., 1981. "Which tetrahedra fill space?". *Mathematics Magazine,* ***54***(5), pp. 227–243.

[44] Gardner, M., 1971. *Sixth book of mathematical games from Scientific American*. WH Freeman San Francisco.

[45] Goldberg, M., 1972. "The space-filling pentahedra". *Journal of Combinatorial Theory, Series A,* ***13***(3), pp. 437–443.

[46] Goldberg, M., 1979. "Convex polyhedral space-fillers of more than twelve faces". *Geometriae Dedicata,* ***8***(4), pp. 491–500.

[47] Goldberg, M., 1982. "On the space-filling enneahedra". *Geometriae Dedicata,* ***12***(3), pp. 297–306.

[48] Williams, R. E., 1968. "Space-filling polyhedron: its relation to aggregates of soap bubbles, plant cells, and metal crystallites". *Science,* ***161***(3838), pp. 276–277.

[49] Williams, R., 1979. *The geometrical foundation of natural structure: A source book of design*. Dover New York.

[50] Johnson, N. W., 1966. "Convex polyhedra with regular faces". *Canadian Journal of Mathematics,* ***18***, pp. 169–200.

[51] Alvarez, S., 2017. "The gyrobifastigium, not an uncommon shape in chemistry". *Coordination Chemistry Reviews,* ***350***, pp. 3–13.

[52] Sederberg, T. W., and Greenwood, E., 1992. "A physically based approach to 2–d shape blending". *ACM SIGGRAPH computer graphics,* ***26***(2), pp. 25–34.

[53] Sederberg, T. W., Gao, P., Wang, G., and Mu, H., 1993. "2-d shape blending: an intrinsic solution to the vertex path problem". *Proceedings of the 20th annual conference on Computer graphics and interactive techniques*, pp. 15–18.

[54] Alexa, M., Cohen-Or, D., and Levin, D., 2000. "As-rigid-as-possible shape interpolation". In Proceedings of the 27th annual conference on Computer graphics and interactive techniques, ACM Press/Addison-Wesley Publishing Co., pp. 157–164.

[55] Turk, G., and O'brien, J. F., 2005. "Shape transformation using variational implicit functions". In ACM SIGGRAPH 2005 Courses, ACM, p. 13.

[56] Rao, M., 2017. Exhaustive search of convex pentagons which tile the plane. arXiv preprint arXiv:1708.00274.


Copyright © 2020 by ASME

[57] Grünbaum, B., and Shephard, G. C., 1987. *Tilings and patterns*. Freeman.

[58] Akleman, E., Chen, J., and Meric, B., 2000. "Web-based intuitive and effective design of symmetric tiles". *Proceedings of ACM Multimedia,* ***21***(4), pp. 100–108.

[59] Srinivasan, V., Akleman, E., and Chen, J., 2002. "Interactive construction of multi-segment curved handles". In 10th Pacific Conference on Computer Graphics and Applications, 2002. Proceedings., IEEE, pp. 429–430.

[60] Liu, Y., and Collins, R., 1999. "Frieze and wallpaper symmetry groups classification under affine and perspective distortion".

[61] Bérczi, S. "Katachi u symmetry in the ornamental art of the last thousands of years of eurasia".

[62] Chung, P. N., Fernandez, M. A., Li, Y., Mara, M., Morgan, F., Plata, I. R., Shah, N., Vieira, L. S., and Wikner, E., 2012. "Isoperimetric pentagonal tilings". *Notices of the AMS,* ***59***(5).

[63] Chavey, D., 1989. "Tilings by regular polygons—ii". *Computers Mathematics With Applications - COMPUT MATH APPL,* ***17***, 12, pp. 147–165.

[64] Y.T., Z., and X.L., W., 2018. "Ductility and plasticity of nanostructured metals: differneces and issues". *Maeritals Today Nano,* ***2***, pp. 15–20.

[65] Seepersad, C. C., Haberman, M. R., and Morris, C. B., 2019. "Design exploration of additively manufactured metamaterials". *The Journal of the Acoustical Society of America,* ***146***(4), pp. 2757–2757.

[66] Correa, D. M., Seepersad, C. C., and Haberman, M. R., 2015. "Mechanical design of negative stiffness honeycomb materials". *Integrating Materials and Manufacturing Innovation,* ***4***(1), p. 10.

[67] Correa, D. M., Klatt, T., Cortes, S., Haberman, M., Kovar, D., and Seepersad, C., 2015. "Negative stiffness honeycombs for recoverable shock isolation". *Rapid Prototyping Journal*.



Copyright © 2020 by ASME